OPTICAL REVIEW Vol. 6, No. 4 (1999) 293–301

Fractal Roughness Retrieval by Integrated Wavelet Transform

Aristide DOGARIU,[1,4] Glenn BOREMAN,[1,5] Jun UOZUMI,[2,6,*] and Toshimitsu ASAKURA[3]

[1]*School of Optics/CREOL, University of Central Florida, Orlando, Florida 32816, USA,* [2]*Research Institute for Electronic Science, Hokkaido University, Sapporo, Hokkaido, 060-0812 Japan,* [3]*Faculty of Engineering, Hokkai-Gakuen University, Sapporo, Hokkaido, 064-0926 Japan*

(Received January 4, 1999; Accepted March 12, 1999)

An integrated-wavelet-transform (IWT) approach is proposed for the study of scattering from slightly rough surfaces that manifest scaling properties over a finite domain of correlation lengths. Instead of collecting angle-resolved intensities, values of the irradiance integrated over increasing areas are used to enhance the contributions of small irradiances at large scattering angles and to reduce the coherent noise. In the case of self-similar surfaces, the scaling behavior of IWT allows investigation of the surface roughness at various length scales. For the realistic case of self-affine surfaces, IWT permits the evaluation of the scaling exponent of the autocorrelation and also offers a direct way to evaluate the necessary length scale of the surface profile.

Key words: Integrated wavelet transform, rough surface, fractal surface, self-similar surface, self-affine surface, autocorrelation, scaling exponent

1. Introduction

Scattering from moderately rough surfaces is an area of active interest.[1)] Most of the surfaces in the industrial environment can be easily brought into this regime by adjusting the wavelength of the radiation used for their inspection. In this regime, a quite accurate description of the scattering phenomena is obtained by means of the scalar Kirchhoff diffraction theory. The light scattered from a slightly rough surface is considered as a sum of a coherent and a diffuse component. The coherent term represents the spread function of the input aperture multiplied by a constant depending on the variance σ of the surface height variation, while the diffuse component depends not only on σ but also on the autocorrelation function (ACF) of the surface height variations. As long as a detailed description of the surface is needed, the attention is pointed toward the diffuse component of the scattered field.

On the basis of light scattering measurements, there are two different ways to provide a surface roughness description. First, we can compare directly the angle-resolved scattering data with roughness-model-dependent theories. This is a direct and easy way to characterize a surface however, one must make initial assumptions about the ACF. Second, starting with the values of the scattered intensity one can solve the inverse problem and describe the surface statistics without any initial assumption about ACF.[2,3)] Whatever alternative we choose, the starting point of the analysis is the collection of experimental data and, therefore, the description of the surface roughness is practically determined by the quality of the angular-resolved scattering data. In spite of a correct understanding of the phenomenon of light scattering from slightly rough surfaces, there are still serious implementation and reliability problems for optical scattering techniques.

In the case of gently rough surfaces, the intensities in the diffuse component are several orders of magnitude weaker than the specular component. Moreover, the description of the angular-dependent scattered intensities requires an investigation over as large an angular domain as possible. Consequently, the weak intensities of the diffuse component should be scanned over a wide dynamic range and this imposes serious experimental limitations for the detection system. Usually, one is required to normalize the relative sensitivities of the detection system at different scattering angles. Beside the sensitivity requirement, the speckle noise affects significantly the variation of the intensity for small changes of the scattering angle. There is always a need to average out this effect by enlarging the detector aperture, at the expense of the angular resolution, or by moving the sample and/or the detector while taking a large number of scattering data. Another practical difficulty arises when the investigated surface is not isotropically rough. The attempts to average out the speckle effect should be, in this case, carefully correlated to the directional features of the surface.

We earlier proposed to solve some of these problems by making integrated irradiance measurements instead of collecting the real angle-resolved intensities.[4,5)] In the Fourier transform plane, the measurement of the integrated irradiance through filters of increasing area enhances the contribution of small intensities at large scattering angles and, meanwhile, completely eliminates the undesired speckle noise. Based on Kirchhoff's scalar the-

[4]also with Physics Department, Transylvania University, Brasov 2200, Romania.

[5]also with Electrical Engineering Department, University of Central Florida, Orlando, Florida 32826, USA.

[6]Present address: Faculty of Engineering, Hokkai-Gakuen University, Sapporo, Hokkaido, 064-0926 Japan.

*E-mail: uozumi@eli.hokkai-s-u.ac.jp

ory, a theoretical dependence was developed for the integrated irradiance as a function of filter magnification.[5] This approach provided a satisfactory agreement with the description of rough surfaces given by mechanical profilometer.

It was later recognized[6] that the proposed method for measurement and interpretation of scattering data can be described in terms of the two-dimensional wavelet transform[7,8] of the surface height variations. We demonstrated that, through an inversion of the integrated wavelet transform (IWT), the ACF can be evaluated from the values of the integrated irradiance in the Fourier plane.[6] It should be emphasized here that, being based on the same scattering theory, the inversion procedure in terms of IWT cannot bring additional information about the scattering surfaces in comparison to the inversion of angular-resolved scattering data. However, in solving the Fredholm equation of the first kind associated to the inverse problem, the reliability of a solution directly depends on the quality of experimental data. In order to recover the ACF by the IWT procedure, one uses the integrated irradiance, a smooth and monotonic function rather than a stepwise one.[9] This is not an alternative approach to the scattering problem but a way to use and interpret the values of the integrated irradiance. Note that, in the IWT procedure, an asymmetrical wavelet and its subsequent rotation can also solve the problem of anisotropic roughness which cannot be tackled by a conventional approach.

In the present paper, the IWT approach is applied to the particular case of fractal surfaces. When surfaces are so irregular that geometrical concepts such as the surface area cease to be practically meaningful, the geometry of fractals provides a useful framework for surface description.[10] Deviations from an ideal planar surface can be adequately described in terms of a fractal surface with $2<D<3$. A wide variety of surfaces and interfaces are well represented by the roughness associated with self-similar or self-affine processes. Fractals, and in particular fractal surfaces, are objects manifesting invariance to scale transformations. No characteristic length scale exists and, upon magnification, a fragment looks similar (in the mean) to the whole. Consequently, scaling-oriented techniques, such as the wavelet transformation, may offer an easier and more direct description of fractal roughness.

In Sect. 2, the IWT is introduced as a mathematical technique which can resolve independently both position and scale and is further adapted to the case of scattering from slightly rough surfaces. In the next section, the scaling behavior of the ACF of self-similar surfaces is described in the frame of IWT approach. The more general case of self-affine surfaces is studied in Sect. 4. These surfaces manifest a natural cutoff of fractality which is directly monitored by IWT. The scaling properties of IWT are discussed in connection with the shape of the analyzing wavelet. An example of IWT inversion is presented in Sect. 5. The retrieval of surface autocorrelation function from the values of the integrated irradiance is compared to the result of an inverse Fourier transform applied to the angular-resolved scattered intensities. In the last section, some conclusions of this study are pointed out.

2. Integrated Wavelet Transform

The two-dimensional WT of an input function $f(\mathbf{x})$ with respect to the wavelet $g(\mathbf{x})$ is defined as

$$T_f(a, \mathscr{R}, \mathbf{b})=\frac{1}{a^2}\int g^*(a^{-1}\mathscr{R}^{-1}(\mathrm{x}-\mathbf{b}))f(\mathbf{x})d\mathbf{x}$$
$$=\frac{1}{(2\pi)^2}\int \hat{g}^*(a\mathscr{R}^{-1}\mathbf{k})\hat{f}(\mathbf{k})\exp(i\mathbf{bk})d\mathbf{k}, \quad (1)$$

where the symbols * and $\hat{}$ stand for the complex conjugate and an operation of the Fourier transform, respectively, while $1/a$, $\mathscr{R}$, and $\mathbf{b}$ indicate the magnification, the rotation, and the position in the WT domain, respectively. The rotation operator $\mathscr{R}=\mathscr{R}(\theta)$ is defined by

$$\mathscr{R}(\theta)=\begin{pmatrix}\cos\theta & -\sin\theta\\ \sin\theta & \cos\theta\end{pmatrix}. \quad (2)$$

In performing the transformation defined in Eq. (1), no information about $f(\mathbf{x})$ is lost, and this relation can be inverted as long as the wavelet admissibility condition, namely

$$\frac{1}{(2\pi)^2}\int\frac{|\hat{g}(\mathbf{k})|^2}{|\mathbf{k}|^2}d\mathbf{k}<\infty, \quad (3)$$

is satisfied. This requires that at least the first moment of g is zero, namely $\int_0^\infty g(x)dx=0$, and that the wavelet function decreases more slowly than $x^{1/2}$ as $x\to 0$.[6] This admissibility condition implies that the wavelet is restricted around the origin.

The irradiance in the WT plane can be integrated. An IWT, defined as a function of the wavelet magnification $1/a$ and the wavelet rotation θ, can be written as

$$I(a, \theta)=\int |T_f(a, \mathscr{R}, \mathbf{b})|^2 d\mathbf{b}. \quad (4)$$

Using Parseval's theorem, the integral can be evaluated in the filter plane and it can be shown that[6]

$$I(a, \theta)=\frac{1}{a^2}\int G^*\left(\frac{\mathscr{R}^{-1}\mathbf{x}}{a}\right)F(\mathbf{x})d\mathbf{x}, \quad (5)$$

where G and F stand for the two-dimensional autocorrelation functions of the wavelet $g(\mathbf{x})$ and input $f(\mathbf{x})$, respectively.

This general formalism can be easily adapted to the case of slightly rough surfaces when just a small phase modulation of the complex scattered amplitude is introduced by scattering on the surface.

The topography of a rough surface can be described by the height $z(\mathbf{x})$, measured from a reference plane S, as a function of the lateral position $\mathbf{x}$. The roughness of the surface is described, therefore, by the statistical distribution of the heights $z(\mathbf{x})$. Usually, a Gaussian distribution

of heights is assumed for the theoretical description of the roughness.[11] However, this description refers to the *vertical* characteristic of the surface and does not take into account the *horizontal* length scales involved in a surface profile. To appreciate how the height $z(\mathbf{x})$ varies on the *horizontal* plane, the profile autocorrelation function is used. If we restrict our comments to the case of isotropic surfaces, the normalized autocorrelation function is defined as[8]

$$C(x)=\sigma^{-2}\langle z(x'+x)z(x')\rangle, \tag{6}$$

where $\langle\cdots\rangle$ denotes an ensemble average over all choices of the origin on the surface. By assuming that $\langle z(x)\rangle=0$, the rms roughness σ is given by

$$\sigma=\sqrt{\langle z^2(x)\rangle}. \tag{7}$$

When a plane wave with the wavelength λ illuminates a rough surface and if $kz(x)<1$, the diffuse component of the intensity distribution scattered in the far-field region is well approximated by a Fourier transform of the autocorrelation function $C(x)$ of the surface height variation $z(x)$ multiplied by its variance,[5,6]

$$I_{\text{diff}}(k)\propto\sigma^2\hat{C}(x). \tag{8}$$

We can consider that, for the special case of a slightly rough surface, the input function for the IWT analysis corresponds to $z(\mathbf{x})$ and, consequently, the function F of Eq. (5) corresponds to autocorrelation C defined in Eq. (6). In this case, Eq. (5) represents the relationship between the integrated irradiance of the scattered light in the far field and the surface height variation and is an extension of the classical result of Eq. (8). The IWT approach has been applied to slightly rough surfaces with Gaussian and negative exponential autocorrelation functions. Well-defined maxima were found for the integrated irradiance as a function of the magnification parameter of the WT.[6] The presence of this maximum is explained by considering the wavelet transformation as a kind of mathematical *microscope* used to observe an image of the input. In the present example, its *magnification* is defined by the parameter a while its impulse response is described by the wavelet shape. In this respect, the maximum in the dependence of I versus a is equivalent to the *focus* position of the *microscope*. There is an optimum magnification of the microscope at which the characteristic length scale of the profile L is matched to the impulse response size and, consequently, $I(a)$ becomes maximum. From the position of this maximum, as a function of magnification, the surface autocorrelation length L can be extracted.

Because the admissibility condition is satisfied, Eq. (5) can be inverted and the autocorrelation function of the surface profile can be evaluated from the values of the integrated intensity in the WT plane. This represents a new approach to the inverse problem associated to scattering from slightly rough surfaces.

In the next sections, IWT will be applied for the specific case of light scattering from surfaces with fractal-like characteristics.

3. Self-Similar Surfaces

If a surface lies in the three-dimensional Euclidean space and if we try to cover it with squares of the linear dimension l, it may happen that the number N of required squares depends on the size of the squares in such a way that

$$D\equiv\lim_{l\to 0}\frac{\log N(l)}{\log l} \tag{9}$$

is finite and non-integer. All the information about the surface is contained in the value D of this limit, called the fractal or Hausdorff dimension of the surface.[9] The finiteness of this limit implies, for $l\to 0$, a scaling like

$$N\propto l^{-D},\quad 2<D<3. \tag{10}$$

This approach for the description of a surface is usually called the definition of the surface dimension in terms of *tiling*.[12] If Eq. (10) is valid, the surface is self-similar and its irregularity, as compared with a plane square, is fully measured by the fractal dimension D. Of course, this is true only in an averaged sense and, for a rough surface, the concept of statistical self-similarity is more appropriate. By increasing the resolution of a covering process (i.e., by reducing the yardstick l), the same statistical properties are revealed for such a rough surface. A value of $D=2$ corresponds to a perfectly *smooth* (but not necessarily flat) surface, while a value of $D=3$ means a space-filling surface which is indistinguishable from a uniform distribution of *mass* in the three-dimensional space.

For self-similar surfaces, no definite scale length on the surface profile exists, and we can expect that a correlation function like $C(x)\propto x^{-\alpha}$ may be used to describe the surface roughness. The parameter α is just a generic exponent describing, in terms of the autocorrelation function, the invariance to scale transformation: $C(\gamma x)\propto\gamma^{-\alpha}C(x)$. This kind of scaling autocorrelation function has been successfully used to describe porous coal surfaces,[13] mesoporous silica gels,[14] or heterogeneous chemically active surfaces.[15] Of course, for real surfaces, this scaling form of $C(x)$ is valid only for a range of x limited by the microscopic properties of the surface and by the inherent finite extent of the sample. However, for the case of self-similar surfaces, the IWT approach leads to some interesting results.

Let us consider the wavelet transformation defined in Eq. (5) restricting our consideration to the case of isotropic functions. Using the proposed scaling form for the autocorrelation function, Eq. (5) becomes

$$I(a)=a^{-2}\int_0^\infty G^*\left(\frac{x}{a}\right)x^{-\alpha}x\,dx. \tag{11}$$

We now identify how the scaling form of $C(x)$ determines the IWT behavior through Eq. (11). By making the change of variable as $x=ax'$, Eq. (11) can be written as

$$I(a)=a^{-2}\int_{0+}^{\infty} G^*(x')(ax')^{-\alpha}a^2x'dx'$$
$$=a^{-\alpha}\int_{0+}^{\infty} G^*(x)x^{-\alpha+1}dx, \tag{12}$$

where the singularity at $x=0$ has been omitted. Obviously, the behavior of $I(a)$ is determined by the scaling exponent α of the autocorrelation function and by the behavior of the wavelet autocorrelation function $G(x)$ for, respectively, small and large values of the argument x.

Recalling the wavelet admissibility condition of Eq. (3), we can assume that the wavelet function decreases at infinity like x^{-m} with an exponent $m>0$ and, in such conditions, Eq. (11) becomes

$$I(a)=a^{-\alpha}\int_{0+}^{\infty} x^{-m}x^{-\alpha+1}dx. \tag{13}$$

A brief inspection of Eq. (13) reveals two different possibilities. First, if $\alpha>1-m$, then the integral over x is finite and the integrated intensity scales like $a^{-\alpha}$. Second, if $\alpha<1-m$, then the integral diverges in general but, in the limit of large magnifications, such as when $a\to 0$, we have

$$I(a)\approx a^{-\alpha}\int_{0+}^{1/a} x^{1-m-\alpha}dx\propto a^{m-2}. \tag{14}$$

Accordingly, the IWT follows the scaling behavior of the autocorrelation function only under certain conditions. If the scaling exponent α of the autocorrelation function and the exponent m describing the shape of the wavelet satisfy the condition $\alpha>1-m$, the integrated intensity scales like $I(a)\propto a^{-\alpha}$. Otherwise, the scaling takes the form of $I(a)\propto a^{m-2}$. Some rigorous results about scalings and wavelets can also be found in Holshneider.[16]

A *Mexican-hat* wavelet, illustrated in Fig. 1(a), is described as

$$g(x)=(2-|\mathbf{x}|^2)\exp\left(-\frac{|\mathbf{x}|^2}{2}\right) \tag{15}$$

and approximated in the Fourier plane (Fig. 1(b)) by

$$|\hat{g}(k)|^2=\begin{cases}1 & \text{if } k_1<k<k_2\\ 0 & \text{otherwise}\end{cases} \tag{16}$$

where k_1 and k_2 are constants to be chosen arbitrarily. For this particular wavelet, a straightforward integration of Eq. (11) results in

$$I(a)\propto\left(\frac{k_1}{a}\right)^{\alpha}, \tag{17}$$

for $0<\alpha<2$.

This scaling property of $I(a)$ can also be demonstrated by analyzing the integrated intensity in a diffraction experiment. Suppose that the behavior of the irradiance in the Fourier plane is like $k^{-\kappa}$, and that no restriction is imposed on the exponent κ except that $\kappa>0$. $I(a)$ is given by a two-dimensional integration of the intensity with scattering vectors $\mathbf{k}$ satisfying $(k_1/a)<k<(k_2/a)$. By a direct integration, we obtain

$$I(a)\propto\int_{k_1/a}^{k_2/a} k^{-\kappa}k\,dk\propto\left(\frac{k_1}{a}\right)^{2-\kappa}. \tag{18}$$

For $\kappa<2$, the last result is identical with Eq. (17) if $2-\alpha=\kappa$, which, in fact, is the usual relationship between the scaling exponents of the autocorrelation function and the power spectrum in the case of a two-dimensional Fourier transform. For $\kappa>2$, the power spectrum vanishes quicker than the area of integration and, consequently, the integrated intensity decreases when the magnification $1/a$ is increased.

In conclusion, a study of the scaling behavior of the integrated irradiance as a function of a can be used, under certain conditions, to infer the scaling exponent of the autocorrelation function. As previously indicated, as long as no correlation length is assumed for the surface roughness, the wavelet *microscope* cannot match a length scale and, accordingly, no maximum exists for $I(a)$. The finite extension L of the surface correlations can be accounted for by a multiplicative exponential factor $\exp(-x/L)$ in the form of $C(x)$ in a similar manner to that used in criti-

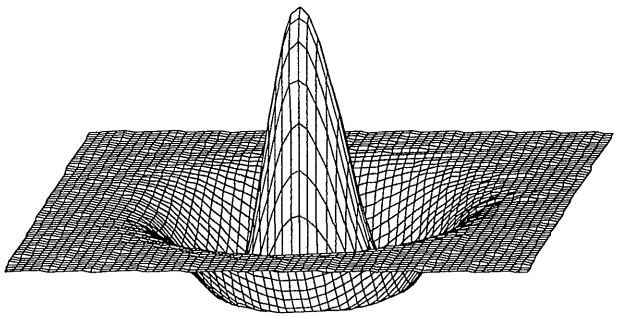

(a)

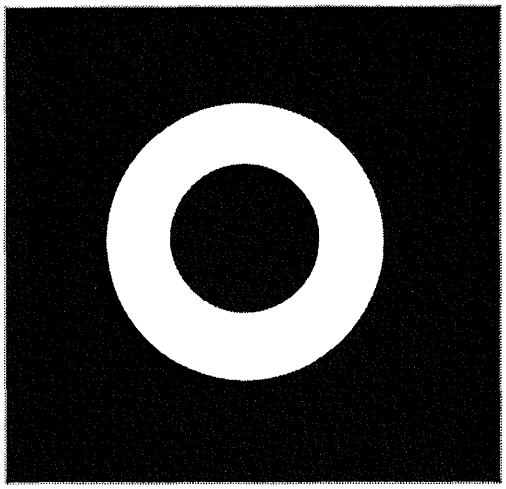

(b)

Fig. 1. (a) Shape of the two-dimensional *Mexican-hat wavelet*. (b) An approximate (band-pass filter) of the Fourier transform of the wavelet in (a).

cal phenomena or in the studies of scattering from fractal aggregates.[17] L has the significance of an effective cutoff of the fractal regime. However, including this form of $C(x)$ in the present analysis will not modify the scaling properties of IWT.

4. Self-Affine Surfaces

In the previous section, we considered surfaces that exhibit scale invariance. However, in the process of generating a rough surface, we need not assume similar statistics on directions parallel and normal to the surface. The two directions are physically distinct, and therefore may have different scaling features. The result is a more complex kind of rough surface called a statistically self-affine surface. A typical example is the altitude $z_H(t)$ of a straight-line hiker as a function of time when he walks at constant speed. The function $z_H(t)$ is statistically self-affine if, when t is scaled by γ, z_H is scaled by γ^H.[12] In this case, the definition of a fractal dimension is not straightforward as in the case of self-similar surfaces.[12,18] However, most natural phenomena (clouds, mountains, or sea surfaces) can be modeled using the concept of self-affine surfaces.[18–22]

For a self-affine surface, the mean square increment of the height $z(\mathbf{x})$, that is the structure function,[12] scales like[18–23]

$$S(|\mathbf{x}|)\equiv\langle[z(\mathbf{x}_2)-z(\mathbf{x}_1)]^2\rangle\propto|\mathbf{x}_2-\mathbf{x}_1|^{2H}, \tag{19}$$

where, again, $\langle\cdots\rangle$ denotes an average over all the choices of the origin for two position vectors $\mathbf{x}_1$ and $\mathbf{x}_2$. The exponent $0<H<1$ is the Hurst exponent and describes the statistical behavior of the surface. It is important to note that Eq. (19) does not invalidate the usual assumption of Gaussian statistics for the surface heights. Equation (19) expresses the scaling property of the *horizontal* roughness[21] but is not a constraint for the height statistics. For isotropic surfaces, Eq. (19) becomes, by putting $x_1=x'$ and $x_2=x'+x$,

$$S(x)=\langle[z(x'+x)-z(x')]^2\rangle=Ax^{2H},\quad 0<H<1. \tag{20}$$

The physical meaning of the constant A will be apparent in the following. It is easy to see that the mean-square slope behaves as follows: $\lim_{x\to\infty}S(x)/x^2\to 0$. At large scales the surface looks essentially smooth. However, at smaller scales the surface can be regarded as a fractal with the fractal dimension[18,22] given by $D=3-H$. Although the surface described by Eq. (20) is nondifferentiable, the chords joining points separated by a given distance x do have a finite mean-square slope. This may be used further to define a scale length on the structure of the surface. The distance β over which the chord has a unit rms slope,

$$\left\langle\left[\frac{z(x'+\beta)-z(x')}{\beta}\right]^2\right\rangle\equiv 1, \tag{21}$$

is called the *topothesy*[18] of $z(x)$ and can be expressed as[14,19]

$$\beta=A^{1/2(1-H)}=A^{1/2(D-2)}. \tag{22}$$

β may also be called the *strength* of the fractal surface because it represents the resolution of a measurement of $z(x)$ resulting in a rms slope of one radian. Intuitively, an *ideal* measurement on a fractal surface would result in an infinitely large rms slope.

For smooth surfaces described by $D=2$ or equivalently $H=1$, there is no topothesy and

$$\lim_{x\to 0}\frac{S(x)}{x^2}=\delta^2, \tag{23}$$

where δ^2 is the mean square slope. Making use of Eqs. (20) and (22), the structure function of the fractal surface can be written as a function of the fractal dimension D as

$$S(x)=\beta^{2D-4}x^{6-2D}\quad 2<D<3. \tag{24}$$

As can be seen from Eqs. (22) and (24), the topothesy and the structure function of a self-affine surface definitely depend on the fractal dimension.

Note that the proportionality constant in Eq. (20) depends on the specific properties of the surface profile. A is a function of a scale length on the surface profile, β, and also a function of the scaling parameter H:

$$A=\beta^{2(1-H)}. \tag{25}$$

The complex character of self-affine surfaces is evident; the parameters describing the surface, H and β, act not only on the scaling part of Eq. (20) but also on the value of the proportionality constant A.

So far, we used the structure function $S(x)$ to describe the topography of a self-affine surface because it has the appealing quality of being independent of the position of the plane from which $z(x)$ is measured and, meanwhile, describes the appropriate scaling properties of self-affine rough surfaces. Unfortunately, $S(x)$ does not appear explicitly in the theories of wave scattering, and therefore the equivalent approach in terms of the surface autocorrelation function of Eq. (6) must be used. For stationary rough surfaces, $S(x)$ and $C(x)$ are related by[11]

$$S(x)=2\sigma^2[1-C(x)]. \tag{26}$$

Rigorously speaking, $S(x)$ can diverge at infinity for self-affine processes and the stationarity condition is never reached. However, fractal profiles represent an idealization of real physical surfaces. The divergence of $S(x)$ at large x (or the corresponding divergence of the power spectrum at low frequencies) is unphysical and the actual roughness measurement converts this quantity into a finite one.[10] In practice, the rms roughness saturates, for sufficiently large horizontal distances x, at a certain value σ.[24] The existence of a cutoff L of the fractality can be included in an autocorrelation function such as

$$C(x)=\sigma^{-2}\exp\left[-\left(\frac{x}{L}\right)^{2h}\right]. \tag{27}$$

When the surface is measured using a profilometer, the cutoff L can result from experimental effects not directly

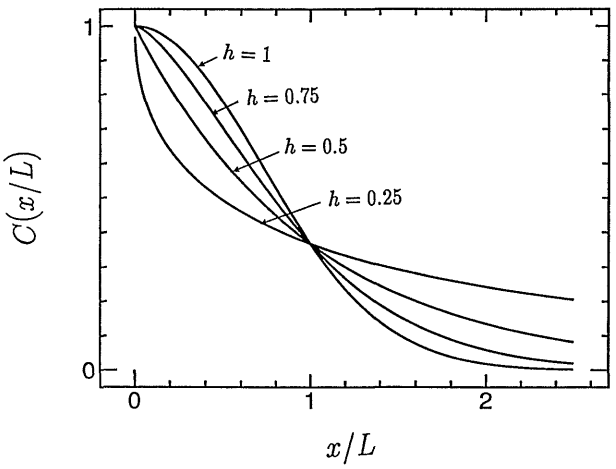

Fig. 2. Autocorrelation functions as defined in Eq. (27) plotted for values of the parameter h as indicated.

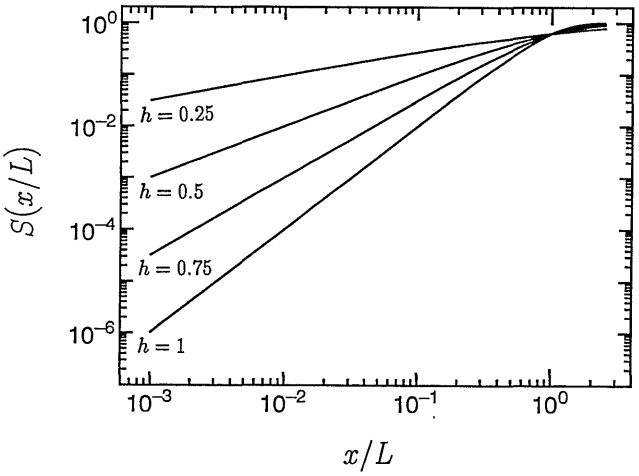

Fig. 3. Structure functions corresponding to the correlation functions in Fig. 2. For small values of the normalized distances x/L, the slopes have the expected values of $2h$.

related to the surface itself. These include[1] the finite size of the investigated area and the detrending process used to remove setup errors (piston, tilt, curvature) from the experimental data. These effects generate a cutoff in the scaling form of a measured power spectrum.[24-26] Also, it was suggested that some particularities of the scattering experiments[10,27] may be explained by such a form for the autocorrelation function of the surface. Being a realistic form of the autocorrelation function, it recovers the traditional Gaussian shape for $h=1$ and the negative exponential for $h=0.5$ (see Fig. 2). The corresponding structure function is given by

$$S(x)=2\sigma^2\left\{1-\exp\left[-\left(\frac{x}{L}\right)^{2h}\right]\right\}. \tag{28}$$

Note that, deep inside the fractal domain (for $x \ll L$), $C(x)$ of Eq. (27) can be approximated by $1-(x/L)^{2h}$ and, accordingly, $S(x)$ has the same form as in Eq. (20) with $h=H$. This is illustrated in Fig. 3, where the structure function corresponding to a correlation function as defined in Eq. (27) is plotted against the normalized distance x/L. As can be seen, for $x/L<0.1$, the structure function has a definite power law behavior with a slope $2H$. We may conclude that a surface having a correlation function as defined in Eq. (27) is a self-affine surface for sufficiently small length scales. Furthermore, using Eqs. (24) and (28), the correlation length L can be expressed in terms of the topothesy T and the fractal dimension D as

$$L=(\sqrt{2}\,\sigma)^{1/(3-D)}\beta^{(2-D)/(3-D)}. \tag{29}$$

Accordingly, we reach the conclusion that, for a fixed σ, the finer the structure on the surface (in other words, the smaller the topothesy), the longer the extension L for the surface correlation.

Being in possession of a reasonable form for the autocorrelation function, we can apply the wavelet transform approach for the case of self-affine surfaces. For example, in the easiest case of a *Mexican-hat* wavelet, the

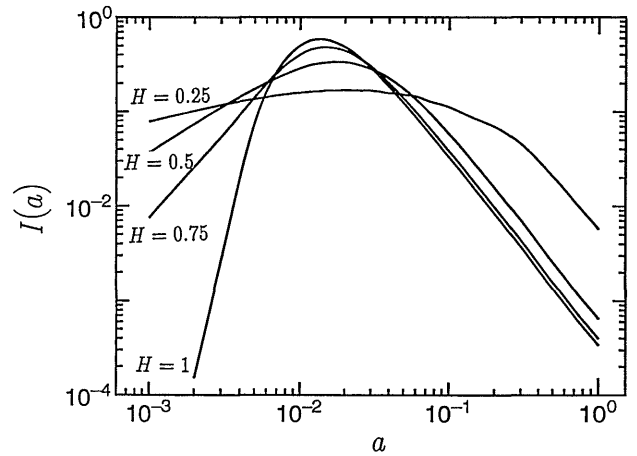

Fig. 4. Integrated irradiance corresponding to self-affine surface described by different values of the Hurst parameter H, as a function of the magnification parameter a. The shape of the analyzing wavelet and the correlation length are the same for all the cases.

autocorrelation function of Eq. (27) can be used in the general form of the integrated irradiance expressed by Eq. (5). Analytical expression cannot be derived in the case of an arbitrary H and results of numerical integration are presented in Fig. 4.

As can be seen, at very small magnifications, such as in the limit $a\to\infty$, the curves corresponding to different H's tend to an asymptotic a^{-2} dependence. We can understand this by imagining that, at these small magnifications, the mathematical *microscope* of the WT cannot distinguish between different kinds of surfaces. As long as the largest length scale on the surface (the correlation length L) cannot be resolved, all the surfaces look essentially smooth. For large a, $I(a)$ is also independent of the shape of the analyzing wavelet. In terms of the mathematical *microscope* at small magnifications, the recorded

signal is obtained by integrating a constant irradiance distribution disregarding the specific choice of the point-spread function. As for the absolute value of 2 for the scaling exponent, this can be explained by following the same argument used to derive Eq. (18). The integration domain corresponds now to scattering vectors with $k \ll 1/L$ where the intensity distribution is essentially constant. A straightforward integration as in Eq. (18) leads to the a^{-2} dependence of the integrated irradiance.

Following a similar explanation, the behavior of $I(a)$ at large magnifications (in the limit $a \to 0$) can be made transparent. First, we must remark that a smoother surface corresponding to a higher parameter H has a far-field intensity distribution that vanishes faster at large spatial frequencies k. Noting that a behavior as in Eq. (18) is also expected for the far-field intensity scattered by self-affine surfaces, a higher value of the parameter H corresponds to a higher exponent κ in Eq. (18). Rougher surfaces tend to scatter light over larger angles and, therefore, correspond to a smaller exponent κ in Eq. (18). As can be seen in Fig. 4 and in agreement with the expectations of Eq. (18), $I(a)$ decreases more rapidly at small a in the case of large parameters H. From the scaling feature of the integrated intensity at high magnifications, therefore, it is possible to extract information about the associated fractal dimension $D=3-H$. Finding the explicit dependence of $I(a)$ at small a is, however, equivalent to solving the problem of light scattering from self-affine surfaces. A scaling behavior with the exponent $-\kappa$ for the intensity in the far field is equivalent to a scaling with the exponent $\kappa-2$ for the integrated intensity. The IWT technique cannot bring additional information about the scaling feature but offers an alternative approach which, especially for experimental reasons, may be very attractive. The IWT technique involves an integrated intensity measurement with the inherent increase of signal to be detected. This is to be appreciated particularly in the case of smooth surfaces with a reduced diffuse scattering. Also, the integrated-irradiance nature of the IWT approach minimizes the statistical fluctuations in the recorded intensity from speckle phenomena.

Besides, as we have pointed out, real surfaces (self-similar or self-affine) have limited scaling characteristics. Therefore, it may be useful in some applications to infer a characteristic scale length on a rough surface. This is done very well by our *microscope* which, with an adjustable magnification, can match a scale length on the surface. The ability of IWT to reveal the characteristic length is demonstrated in Fig. 5, where the integrated intensities corresponding to a correlation function with $H=0.75$ and different correlation lengths are presented. The maximum of $I(a)$ corresponds to that magnification which matches the specific wavelet shape to the length scale on the surface. As can be observed, the smaller the correlation length L of the surface roughness, the higher the magnification $1/a$ needed to reveal it. Obviously, the value of a corresponding to a maximum of the integrated intensity is proportional to the size of the correlation length. Note also that the absolute value of L does not affect the scaling properties at smaller distances on the surface. Consequently, the same dependences are found for $I(a)$ at small a in all the cases. Practically, the curves of $I(a)$ are identical in Fig. 5 but shifted horizontally, corresponding to the matching magnifications.

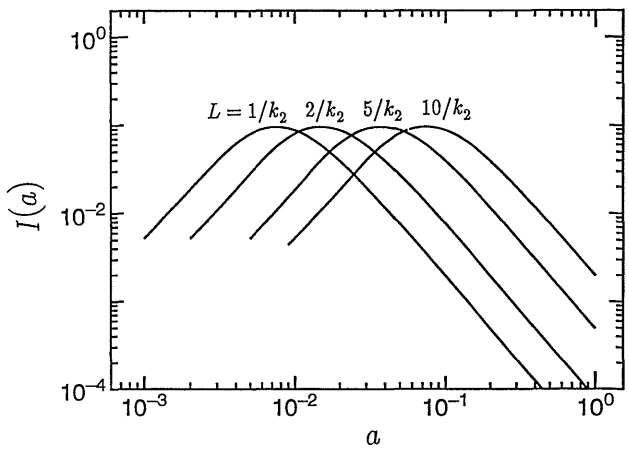

Fig. 5. Integrated irradiance corresponding to self-affine surfaces described by the same parameter $H=0.75$ but having different correlation lengths L, as indicated. The shape of the analyzing wavelet is the same for all the cases.

5. ACF Retrieval

In this section we will briefly present an example of how IWT can be inverted, and therefore applied to retrieve the ACF of the surface fluctuations from the values of the integrated irradiance.

In Fig. 6, two typical profiles of scattered intensities having power-law behaviors are presented. To simulate difficult experimental conditions, the scattering data are strongly corrupted by noise but overall dependences like $k^{-2.25}$ and $k^{-2.75}$, respectively, are evident over an angular domain as large as two decades. The fractal appearance extends down to the spatial frequency $k=1$. Note that, in order to ensure the scaling behavior, the intensities span over more than five orders of magnitude. As we mentioned in the Introduction, in the case of fractal scattering, the need for a large dynamic range of the detection system complicates the acquisition of accurate experimental data.

However, we can integrate the angular-resolved intensity over domains with increasing area as suggested in the IWT approach. By this integration, the necessary dynamic range can be highly reduced and, meanwhile, the speckle noise is drastically diminished. These are proved in Fig. 7, where integrated irradiances, corresponding to the intensities in Fig. 6, are shown as a function of wavelet magnification. Data of Fig. 7 were obtained by using an approximated *Mexican-hat* wavelet having $k_1/k_2=1/3$. Figure 7 clearly shows how this type of measurement can counteract the intensity fall-off, the signal being co-

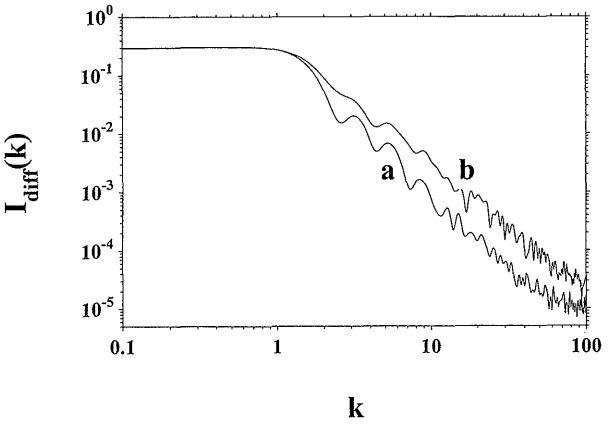

Fig. 6. Angular-resolved values of the scattered intensity. The curves correspond to power-laws with exponent (a) -2.75 and (b) -2.25.

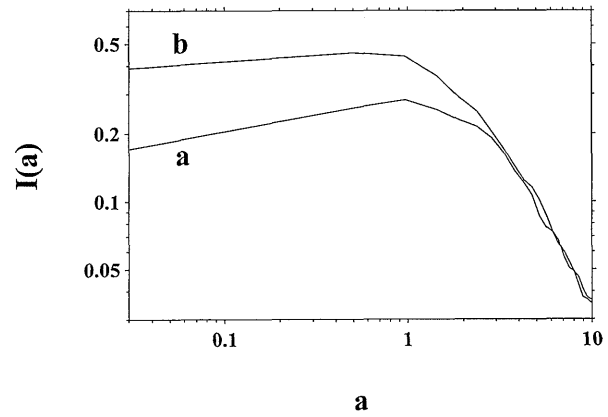

Fig. 7. Integrated irradiance (approximated *Mexican-hat wavelet* with $k_1/k_2=1/3$) corresponding to scattering intensities presented in Fig. 6.

vered with less than two decades of the irradiance variation, and how the speckle noise is practically suppressed. Also visible is the cut-off of the fractal domain. The plateau at small scattering angles, visible in Fig. 6 for $q<1$, generates a maximum in the shape of the integrated irradiance. This time, the cut-off corresponds to a wavelet magnification of $a=1$. For a less than 1, the dependence between the integrated irradiance and the wavelet magnification parameter a can be directly used to infer the power-law behavior of the scattered intensity. The position of the maximum can be used to extract or to control in an automatic procedure the value of the upper cut-off of the fractal domain.

Inverse IWTs were processed for $I(a)$ and are shown in Fig. 8. The result of this inversion, using a dynamic range of only 40 for the magnification parameter a, is presented in Fig. 8 together with the result of an inverse Fourier transform applied to the angular-resolved scattering data of Fig. 6. As can be seen, the power-law behaviors are fully recovered in spite of the low number of $I(a)$

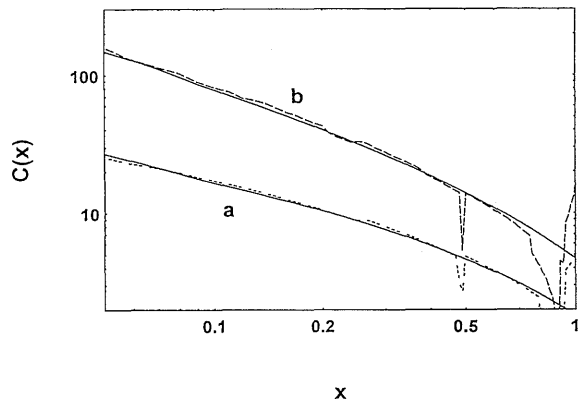

Fig. 8. Autocorrelation functions recovered by inverse IWTs from the values of the integrated irradiance in Fig. 7. Also shown, with dashed lines, are the corresponding autocorrelation functions recovered by inverse Fourier transforms from the values of the angular-resolved intensities presented in Fig. 6.

data and of their relatively reduced dynamic range. The inversion of scattering data by means of IWT is sufficiently close to that provided by the classical Fourier transformation in spite of the fact that their input data are different: the values of the integrated irradiance shown in Fig. 7 for the IWT and, respectively, the angular-resolved intensity shown in Fig. 6 in the case of Fourier transformation. Moreover, the inverse Fourier transformation uses an input with a dynamic range almost three times larger than IWT.

6. Conclusions

Based on the general theory of wavelet transforms, a new approach for the study of the surface roughness was recently introduced. It was demonstrated that the integrated irradiance in the WT plane can be regarded as the WT of the autocorrelation function of the input function and that this relationship can be used to describe the measurement of the integrated intensity scattered by rough surfaces having small height variations. It was also proved that this integrated wavelet transform IWT can be inverted and, consequently, may be used to solve the inverse problem of the scattering from slightly rough surfaces.

In this paper, the IWT approach was applied to the investigation of fractal surfaces with self-similar or self-affine characteristics. The main properties of the self-similar surfaces were reviewed and a scaling-like autocorrelation function was considered. The method based on integrated wavelet transform was applied and the scaling features of the integrated intensity in the WT were investigated. It was demonstrated that the scaling behavior of the IWT follows the scaling of the surface autocorrelation function only in particular cases. Restrictions on the shape of the wavelet and the scaling exponent of the autocorrelation function were pointed out. Because of an appealing practical implementation, the scaling property

was studied for the case of a *Mexican-hat* wavelet.

Self-affine surfaces, a more complex kind of rough surface, were also studied. The parameters that define this type of surface were introduced and it was shown that, in this case, there is a definite scale length on the surface topography. It was demonstrated that a general form of autocorrelation considered describes actually the small scale features of a self-affine surface. This observation emphasizes the general character of the concept of self-affine surfaces. When applied to this particular case, the *microscope* of the IWT easily reveals the characteristic scale length on the surface profile. Given that all real surfaces have at least one characteristic scale length, the ability of the IWT to measure this length is a promising practical advantage of the IWT approach. The scaling behavior of the IWT also reflects the scaling character of the surface structure function.

Finally, the inversion procedure of IWT was tested against the classical method of Fourier transformation of the angular-resolved scattered intensities. The IWT approach uses a much more reduced dynamic range of irradiances while providing a satisfactory solution for the inverse problem associated with the scattering from slightly rough surfaces.

References

1) J. M. Bennett and L. Mattson: *Introduction to Surface Roughness and Scattering* (Optical Society of America, Washington, D.C., 1989).
2) E. Marx, B. Leridon, T. R. Lettieri, J.-F. Song and T. V. Vorburger: Appl. Opt. **32** (1993) 67.
3) P. J. Chandley: Opt. Quantum Electron. **8** (1976) 329.
4) A. Dogariu, M. Dogariu, I. I. Popescu and B. Cosma: Opt. Appl. **19** (1989) 343.
5) A. Dogariu, J. Uozumi and T Asakura: Optik **93** (1993) 52.
6) A. Dogariu, J. Uozumi and T Asakura: Opt. Commun. **107** (1994) 1.
7) A. Grossmann and J. Morlet: *Mathematics and Physics, Lectures on Recent Results*, ed. L. Streit (World Scientific, Singapore, 1985).
8) A. Arneodo, F. Argoul, J. Elezgaray and G. Grasseau: *Nonlinear Dynamics*, ed. G. Turchetti (World Scientific, Singapore, 1988).
9) E. Freysz, B. Pouligny, F. Argoul and A. Arneodo: Phys. Rev. Lett. **64** (1990) 745.
10) E. L. Church: Appl. Opt. **8** (1988) 1518.
11) J. A. Ogilvy: *Theory of Wave Scattering from Random Rough Surfaces* (Adam Hilger, Bristol, 1991).
12) B. B. Mandelbrot: *The Fractal Geometry of Nature* (Freeman, San Francisco, 1982).
13) H. D. Bale and P. W. Schmidt: Phys. Rev. Lett. **53** (1984) 596.
14) D. Rojanski, D. Huppart, H. B. Bale, X. Dacai. P. W. Schmidt, D. Farin., A. Sevi-levy and D. Avenir: Phys. Rev. Lett. **56** (1986) 2505.
15) P. Pfeifer and D. Avenir: J. Chem. Phys. **79** (1983) 3558.
16) M. Holshneider: J. Stat. Phys **50** (1988) 963.
17) J. Teixeira: *On Growth and Form*, eds. H. E. Stanley and N. Ostrowsky (Martinus Nijhoff Publ., Dordrecht, 1986).
18) R. F. Voss: Physica D **38** (1989) 362.
19) R. Glazman and P. B. Weichman: J. Geophys. Res. C **94** (1989) 4998.
20) Y. Agnon and M. Stiassnie: J. Geophys. Res. C **96** (1991) 12773.
21) R. S. Sayles and T. R. Thomas: Nature **271** (1978) 431.
22) B. B. Mandelbrot: J. Stat. Phys. **34** (1984) 895.
23) M. V. Berry and T. M. Blacwell: J. Phys. A: Math. Gen. **14** (1981) 3101.
24) S. K. Sinha, E. B. Sirata and S. Garoff: Phys. Rev. B **56** (1988) 2297.
25) E. L. Church, H. A. Jenkinson and J. M. Zavada: Opt. Eng. **18** (1979) 125.
26) E. L. Church, T. V. Vorburger and J. C. Wayant: Opt. Eng. **24** (1985) 388.
27) E. Marx and T. Vorburger: Appl. Opt. **29** (1990) 3613.